Virucidal properties of metal oxide nanoparticles and their halogen adducts

Johanna Häggström,[a] Denitza Balyozova,[a] Kenneth J. Klabunde*[a] and George Marchin[b]

Received (in Cambridge, MA, USA) 18th September 2009, Accepted 27th November 2009
First published as an Advance Article on the web 2nd February 2010
DOI: 10.1039/b9nr00273a

Selected metal oxide nanoparticles are capable of strongly adsorbing large amounts of halogens (Cl_2, Br, I_2) and mixed halogens. These solid adducts are relatively stable thermally, and they can be stored for long periods. However, in the open environment, they are potent biocides. Herein are described studies with a number of bacteriophage MS2, φX174, and PRD-1 (virus examples). PRD-1 is generally more resistant to chemical disinfection, but in this paper it is shown to be very susceptible to selected interhalogen and iodine adducts of CeO_2, Al_2O_3, and TiO_2 nanoparticles. Overall, the halogen adducts of TiO_2 and Al_2O_3 were most effective. The mechanism of disinfection by these nanoparticles is not completely clear, but could include abrasive properties, as well as oxidative powers. A hypothesis that nanoparticles damage virons or stick to them and prevent binding to the host cell is a consideration that needs to be explored. Herein are reported comparative biocidal activities of a series of adducts and electron microscope images of before and after treatment.

1. Introduction

Numerous studies have clearly demonstrated that solid materials in nanoscale form exhibit unique properties, including enhanced chemical, sorptive, and catalytic properties. Some nanomaterials as solids, slurries, or microemulsions exhibit very effective biocidal properties, including virucidal activity.[1–9] Nanostructured metal oxides can also be effective in filtration media for removing viruses.[10,11]

Studies using free iodine and chlorine dioxide against MS2 and poliovirus have also been reported, and it was concluded that oxidative damage of sulfhydryl groups in the protein coat was an important aspect in the killing mechanism.[12,13]

It is important that more effective broad spectrum biocides be elucidated, especially new and effective biocides that are active as solids, water slurries, or as filtration media (pellets or resins). This paper describes a systematic study of a new family of nanometal oxide-halogen and mixed halogen solid adducts that act as biocides against a series of viruses. The perceived advantages of these nanoparticle–halogen adducts compared with other halogen based disinfectants are that they are solids and can be used as powders, pellets, or slurries; they are at least as active as pure halogen gases/liquids, they are storable as solids for long periods and, upon environmental exposure, they eventually degrade to harmless minerals and salts.

2. Experimental methods

2.1 Nanocrystalline biocides employed

Nanocrystals of Al_2O_3, TiO_2, and CeO_2 were purchased from NanoScale Corporation (www.nanoscalecorporation.com) and were treated with elemental halogens and mixed halogens to obtain stable, solid adducts.[14a,b]

[a]*Department of Chemistry, Kansas State University, Manhattan, KS, 66506, U.S.A. E-mail: kenjk@ksu.edu*
[b]*Division of Biology, Kansas State University, Manhattan, KS, 66506*

2.2 Preparation of high titer bacteriophage lysates

A soft agar overlay procedure was used to prepare high titer lysates of the three bacteriophages MS2, φ-X174 and PRD-1. For MS2, φ-X174, and PRD-1, the C3000, B and C strains of *Escherichia coli* were used as host strains. A small amount of chloroform was added to prevent bacterial contamination of the MS2 and φ-X174 lysates. All lysates were stored at 4–8 °C in the refrigerator.

In order to determine the phage concentration of the prepared lysates, as well as of nanoparticle treated material, serial dilutions were performed. The prepared lysates generally yielded 10^8–10^{11} plaque forming units per ml (pfu/ml). All titers were conducted in triplicate and 10^{-5}–10^{-10} dilutions were generally plated to insure appropriate pfu per set of plates.

2.3. Bacteriophage inactivation procedures

All bacterial strains were cultured in TGYE (tryptone 10 g, glucose 10 g, yeast extract 1 g, NaCl 8g, per liter of media). For solid media, 15 g of agar was added. In some phage systems, thiamine and/or $CaCl_2$ was added for growth or phage adsorption.

Typical phage preparations contained approximately 1×10^7–10^{11} pfu/ml. During each experiment, nanoparticles were added to phosphate buffered saline (PBS) to a final concentration of either 10 mg mL^{-1} or 20 mg mL^{-1}. 100 μL bacteriophage (MS2, φ-X174, or PRD-1) was added to each solution, and the mixture was vortexed. Typically, after 5 and 30 min. reaction time, an aliquot of 100 μL was removed from the solution and added to the appropriate *E. coli* host culture solution kept at 47 °C, containing 100 μL *E. coli* in 2.5 ML TGYE soft agar. This mixture was then plated on TGYE complete agar plates and incubated. Each sample was plated in triplicate and the experiment was repeated at least one more time. After 24 h of incubation at 37 °C, plaque forming units were counted, compared to the control count, and log inactivation values were calculated as

follows: log reduction = log (C_o/C) where C_o = initial concentration and C = after treatment.

Although the nanoparticle preparations undergo significant dilution in going from the treated phage preparation to the soft agar overlay (~1 : 250), in order to ascertain toxic effects of the nanoparticle supernatant to the host cells (which would lead to false positive results, due to damaged or unavailable host cells) the following experiment was typically included with phage experiments. Nanoparticles were added to phosphate buffered saline (PBS) to a final concentration of 20 mg mL^{-1}. The solution was treated precisely as phage-treated host cells. In all cases robust lawns of host cells formed in a typical manner.

2.4. Transmission electron microscopy (TEM)

TEM images of the phage treatments were recorded on a Philips CM 100 TEM, operating at 100 kV.

In order to view the virus, the following procedure was performed. Generally 20 μL of virus solution was put on parafilm in a Petri dish. If necessary, the virus solution was diluted in distilled water first. With a pair of forceps, the 300 mesh copper Formvar/carbon grid was carefully floated on top of the drop for one minute. The grid was removed and the edge of the grid was then carefully touched against a filter paper, in order to remove excess virus solution. The grid was floated on top of a 20 μL drop of 2% uranyl acetate for one minute, followed by removal of excess solution against a filter paper. The grid was then imaged under the microscope.

In order to visualize treated virus solutions under the microscope, 200 μL of the virus solution was put into contact with less than 50 mg of NA–Al_2O_3/ICl_3 Plus. The mixture was vortexed and then allowed to interact for 10 min. The mixture was centrifuged for 5 min and 20 μL of the supernatant was imaged under the microscope, using the above described procedure.

3. Results and discussion

3.1. MS2 virus

It is known that many of the common disease producing animal viruses, for example, those that cause influenza and polio, contain RNA as their genetic material.[15] MS2 is one of the most common surrogates of human enterovirus[1] and it is a single stranded and linear RNA (ssRNA) virus that belongs to the Leviviridae family.[16] MS2 phage has been recommended in the past as a model phage for chlorine, ozone and other disinfectant inactivation studies; however it may be unduly sensitive to iodine.

The experiments using the prepared halogen and interhalogen nanoparticle adducts described earlier[14,17] (Al_2O_3, TiO_2, CeO_2 as nanoscale NanoActive® forms, with adsorbed Cl_2, Br_2, I_2, ICl, ICl_3, IBr) were tested against the different bacteriophages using a method described in the literature.[1]

An initial concentration of 20 mg nanoparticles per mL of buffer solution was used to determine if the nanoparticles were virucidal. The 'naked' metal oxides and the halogen adducts were tested. Table 1 shows the results using the different adducts of NA–Al_2O_3 Plus, NA–TiO_2, and NA–CeO_2 against the coliphage MS2 at a 20 mg mL^{-1} nanoparticle concentration. Only the high concentration of the phage was used, in order to distinguish among the various activities of the different adducts to find the most efficient ones. A complete inactivation of the viruses leads to a 7.11 log reduction, so it can be observed that all the prepared halogen and interhalogen adducts of NA–Al_2O_3 Plus displayed a complete inactivation (log-7) of the MS2 phage. Furthermore, NA–CeO_2 and its adducts were tested and the main difference observed between these adducts and those of NA–Al_2O_3 Plus was that the chlorinated adduct of NA–CeO_2 appeared to act in a manner similar to the "naked" metal oxides, displaying low or no activity. This can possibly be explained by the low amount of chlorine present on NA–CeO_2 as compared to NA–Al_2O_3 Plus. Similar to the NA–CeO_2 adducts, the chlorinated adduct of NA–TiO_2 was inefficient along with the "naked" TiO_2. The other halogen and interhalogen adducts of NA–TiO_2 were very efficient, displaying complete inactivation of the phage.

Table 2 summarizes the results using a slightly lower nanoparticle concentration (10 mg mL^{-1}). Again, a complete inactivation of all the phage occurred for most of the halogenated and for all of the interhalogenated adducts, even at this lower concentration of nanoparticles. As expected, the chlorinated adducts of NA–TiO_2 and NA–CeO_2 were not efficient. These results are very promising since relatively high log inactivations were obtained.

TEM images of the control MS2 virus as well as of the nanoparticle treated virus can be seen in Fig. 1. It appears that the virus has been destroyed by the treatment of NA–Al_2O_3/ICl_3 and only nucleic acids and proteins remain in random arrangements.

To summarize, almost all of the prepared halogen and interhalogen adducts displayed a complete inactivation of the MS2

Table 1 Log reduction of MS2 virus by NA–Al_2O_3 Plus, NA–TiO_2 and NA–CeO_2 adducts (20 mg mL^{-1})

	Contact time/min			Contact time/min			Contact time/min	
Nanoparticle formulation	5	30	Nanoparticle formulation	5	30	Nanoparticle formulation	5	30
Phage control	7.11	7.11	Phage control	7.11	7.11	Phage control	7.11	7.11
NA–CeO_2	T.n.t.c[a]	T.n.t.c.	NA–Al_2O_3	T.n.t.c.	T.n.t.c.	NA–TiO_2	T.n.t.c.	T.n.t.c.
NA–CeO_2/Cl_2	T.n.t.c.	T.n.t.c.	NA–Al_2O_3/Cl_2	−7.11	−7.11	NA–TiO_2/Cl_2	T.n.t.c.	T.n.t.c.
NA–CeO_2/Br_2	−7.11	−7.11	NA–Al_2O_3/Br_2	−7.11	−7.11	NA–TiO_2/Br_2	−7.11	−7.11
NA–CeO_2/I_2	−7.11	−7.11	NA–Al_2O_3/I_2	−7.11	−7.11	NA–TiO_2/I_2	−7.11	−7.11
NA–CeO_2/ICI	−7.11	−7.11	NA–Al_2O_3/ICI	−7.11	−7.11	NA–TiO_2/ICI	−7.11	−7.11
NA–CeO_2/IBr	−7.11	−7.11	NA–Al_2O_3/IBr	−7.11	−7.11	NA–TiO_2/IBr	−7.11	−7.11
NA–CeO_2/ICI_3	−7.11	−7.11	NA–Al_2O_3/ICI_3	−7.11	−7.11	NA–TiO_2/ICI_3	−7.11	−7.11

[a] T.n.t.c. = too numerous to count.

Table 2 Log reduction of MS2 virus by NA–Al_2O_3 Plus, NA–TiO_2 and NA–CeO_2 adducts (10 mg mL^{-1})

	Contact time/min			Contact time/min			Contact time/min	
Nanoparticle formulation	5	30	Nanoparticle formulation	5	30	Nanoparticle formulation	5	30
Phage control	7.11	7.11	Phage control	7.11	7.11	Phage control	7.11	7.11
NA–CeO_2	T.n.t.c.[a]	T.n.t.c.	NA–Al_2O_3	T.n.t.c	T.n.t.c	NA–TiO_2	T.n.t.c.	T.n.t.c.
NA–CeO_2/Cl_2	T.n.t.c.	T.n.t.c.	NA–Al_2O_3/Cl_2	−7.11	−7.11	NA–TiO_2/Cl_2	T.n.t.c.	T.n.t.c.
NA–CeO_2/Br_2	−7.11	−7.11	NA–Al_2O_3/Br_2	−7.11	−7.11	NA–TiO_2/Br_2	−7.11	−7.11
NA–CeO_2/I_2	−7.11	−7.11	NA–Al_2O_3/I_2	−7.11	−7.11	NA–TiO_2/I_2	−7.11	−7.11
NA–CeO_2/ICI	−7.11	−7.11	NA–Al_2O_3/ICI	−7.11	−7.11	NA–TiO_2/ICI	−7.11	−7.11
NA–CeO_2/IBr	−7.11	−7.11	NA–Al_2O_3/IBr	−7.11	−7.11	NA–TiO_2/IBr	−7.11	−7.11
NA–CeO_2/ICI_3	−7.11	−7.11	NA–Al_2O_3/ICI_3	−7.11	−7.11	NA–TiO_2/ICI_3	−7.11	−7.11

[a] T.n.t.c. = too numerous to count.

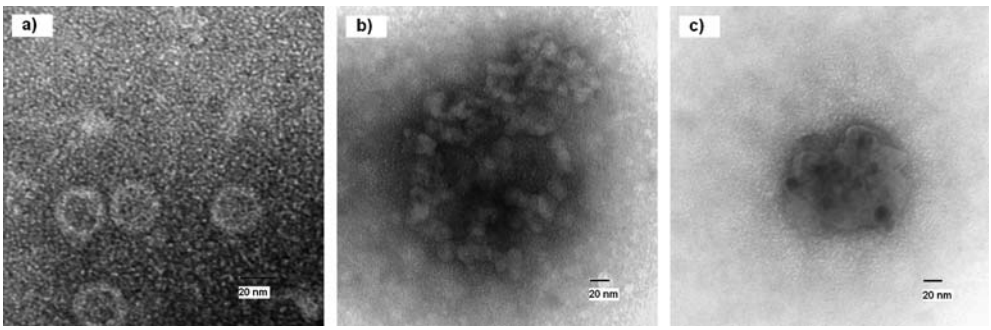

Fig. 1 TEM image of untreated (a) and treated (b and c) MS2 virus.

bacteriophage (corresponding to log-7 kill). MS2 phage may not be a very resistant bacteriophage to chemical disinfection[16] but a log-7 inactivation within 5 min is very impressive. The "naked" metal oxide nanoparticles do not display any detectable activity against the phage, indicating that the oxidizing role of the halogen/interhalogen is extremely important.

3.2. φ-X174 virus

φ-X174 belongs to the Microviridae family.[16] It is a single-stranded DNA virus (ssDNA) whose nucleic acid sequence was determined in 1977 by Fred Sanger and his co-workers. Together with MS2, these two viruses are historic in that they were the first to have their genomes sequenced. The φ-X174 phage has a relatively small genome, containing only 11 genes. The DNA of the φ-X174 phage is circular, which was initially considered very strange and unusual.[15] The spherical phage φ-X174 uses *E. coli* as its bacterial host and it is by far the most widely studied single stranded DNA phage.

An initial concentration of 20 mg nanoparticles per mL of buffer solution was used to determine if the nanoparticles were effective against φ-X174. Table 3 shows the results using the different metal oxide adducts against the coliphage φ-X174 with a nanoparticle concentration of 20 mg mL^{-1}. Immediately it can be seen that the chlorinated adduct of NA–Al_2O_3 Plus is no longer efficient, as it was against MS2 phage and the 'naked' alumina displays no activity. However, all of the other halogenated and interhalogenated adducts of NA–Al_2O_3 Plus displayed

Table 3 Log reduction of φ-X174 virus by NA–Al_2O_3 Plus, NA–TiO_2 and NA–CeO_2 adducts (20 mg mL^{-1})

	Contact time/min			Contact time/min			Contact time/min	
Nanoparticle formulation	5	30	Nanoparticle formulation	5	30	Nanoparticle formulation	5	30
Phage control	7.85	7.85	Phage control	7.85	7.85	Phage control	7.85	7.85
NA–CeO_2	T.n.t.c.[a]	T.n.t.c.	NA–Al_2O_3	T.n.t.c.	T.n.t.c.	NA–TiO_2	T.n.t.c.	T.n.t.c.
NA–CeO_2/Cl_2	T.n.t.c.	T.n.t.c.	NA–Al_2O_3/Cl_2	T.n.t.c.	T.n.t.c.	NA–TiO_2/Cl_2	T.n.t.c.	T.n.t.c.
NA–CeO_2/Br_2	T.n.t.c.	T.n.t.c.	NA–Al_2O_3/Br_2	−7.85	−7.85	NA–TiO_2/Br_2	−7.85	−7.85
NA–CeO_2/I_2	T.n.t.c.	T.n.t.c.	NA–Al_2O_3/I_2	−7.85	−7.85	NA–TiO_2/I_2	−7.85	−7.85
NA–CeO_2/ICI	−7.85	−7.85	NA–Al_2O_3/ICI	−7.85	−7.85	NA–TiO_2/ICI	−7.85	−7.85
NA–CeO_2/IBr	−7.85	−7.85	NA–Al_2O_3/IBr	−7.85	−7.85	NA–TiO_2/IBr	−7.85	−7.85
NA–CeO_2/ICI_3	−7.85	−7.85	NA–Al_2O_3/ICI_3	−7.85	−7.85	NA–TiO_2/ICI_3	−7.85	−7.85

[a] T.n.t.c.. = too numerous to count.

Table 4 Log reduction of φ-X174 virus by NA–Al_2O_3 Plus, NA–TiO_2 and NA–CeO_2 adducts (10 mg mL^{-1})

	Contact time/min			Contact time/min			Contact time/min	
Nanoparticle formulation	5	30	Nanoparticle formulation	5	30	Nanoparticle formulation	5	30
Phage control	−7.85	7.85	Phage control	7.85	7.85	Phage control	7.11	7.11
NA–CeO_2	T.n.t.c.[a]	T.n.t.c.	NA–Al_2O_3	T.n.t.c.	T.n.t.c.	NA–TiO_2	T.n.t.c.	T.n.t.c.
NA–CeO_2/Cl_2	T.n.t.c.	T.n.t.c.	NA–Al_2O_3/Cl_2	T.n.t.c.	T.n.t.c.	NA–TiO_2/Cl_2	T.n.t.c.	T.n.t.c.
NA–CeO_2/Br_2	T.n.t.c.	T.n.t.c.	NA–Al_2O_3/Br_2	−7.85	−7.85	NA–TiO_2/Br_2	−5.57	−4.56
NA–CeO_2/I_2	T.n.t.c.	T.n.t.c.	NA–Al_2O_3/I_2	−7.85	−7.85	NA–TiO_2/I_2	−7.85	−7.85
NA–CeO_2/ICI	T.n.t.c.	T.n.t.c.	NA–Al_2O_3/ICI	−7.85	−7.85	NA–TiO_2/ICI	−7.85	−7.85
NA–CeO_2/IBr	−4.21	−4.93	NA–Al_2O_3/IBr	−7.85	−7.85	NA–TiO_2/IBr	−7.85	−7.85
NA–CeO_2/ICl_3	T.n.t.c.	T.n.t.c.	NA–Al_2O_3/ICl_3	−7.85	−7.85	NA–TiO_2/ICl_3	−7.85	−7.85

[a] T.n.t.c.. = too numerous to count.

a complete inactivation of the φ-X174 phage, corresponding to a log reduction of almost 8. In contrast, the chlorinated, brominated and iodinated adducts of NA–CeO_2 did not display any noticeable activity. This may be explained by the relatively lower loading of halogen on the cerium oxide surface, compared to on NA–Al_2O_3 Plus. Like the NA–CeO_2 and NA–Al_2O_3 Plus adducts, the chlorinated adduct of NA–TiO_2 was not effective, nor was the 'naked' TiO_2. The brominated adduct had a decreased efficiency and did not display complete reduction in the amount of phage. The calculated log reduction was higher during a 5 min interaction compared to the 30 min interaction. Repetitions of the experiment produced the same result. Predictably, however, the other halogen and interhalogen adducts produced effective log inactivations.

Table 4 contains the results with φ-X174 using a 10 mg mL^{-1} concentration of nanoparticles. Similar results were obtained for the alumina adducts: again the chlorinated and 'naked' metal oxides were not efficient, whereas the other adducts displayed excellent activities. For the NA–CeO_2 adducts, even lower activities were observed using this lower nanoparticle concentration; both the ICl and the ICl_3 adducts no longer had a detectable effect, whereas the activity of NA–CeO_2/IBr had significantly decreased. TiO_2 and Al_2O_3 adducts displayed complete inactivations for all the interhalogen adducts and the iodinated adduct. The standard deviation values obtained for the adducts displaying less than complete inactivation were all less than ±0.5.

Based on these findings we note a distinct difference in the effectiveness of the prepared nanoparticles against MS2 and φ-X174, with the former being more susceptible to nanoparticle treatment. A similar observation has been reported in the literature, where iodinated resins were used against MS2, φ-X174, PRD1 and GA virus.[16] Using the more resistant virus φ-X174, we have been able to observe differences in the activities between the adducts prepared from different metal oxide nanoparticles. The adducts prepared from NA–Al_2O_3 Plus were noticeably better than the adducts prepared from NA–CeO_2 or NA–TiO_2. All the adducts prepared from NA–Al_2O_3 Plus, except for the chlorinated adduct, displayed a complete inactivation of the φ-X174 phage, corresponding to a log inactivation of almost 8. The NA–TiO_2 adducts are also very active; however the brominated adduct did not display a complete inactivation of the phage used. The NA–CeO_2 adducts did not perform nearly as well as the already mentioned NA–Al_2O_3 Plus and NA–TiO_2 adducts. Only the interhalogen adducts performed somewhat well, with all of them displaying a complete inactivation at a 20 mg mL^{-1} nanoparticle concentration.

TEM images of the control φ-X174 virus and treated virus (using NA–Al_2O_3/ICl_3 Plus) can be seen in Fig. 2. After treatment it appears that the virus had been destroyed and only nucleic acids and proteins remain in random arrangements. It can be seen that small parts of proteins and nucleic acids appear to form infinite networks together. It is clear that there has been a definite change in the structure of the virus. In Fig. 2c small dark spots, approximately 30 nm in size can be observed. We believe these spots are due to halogen that has remained after the treatment. The spots are very electron dense and halogens would appear dark in a TEM image.

3.3. PRD-1 virus

PRD-1 belongs to the Tectiviridae family and is a lipid-containing virus.[15] It is a very complex membrane-containing double

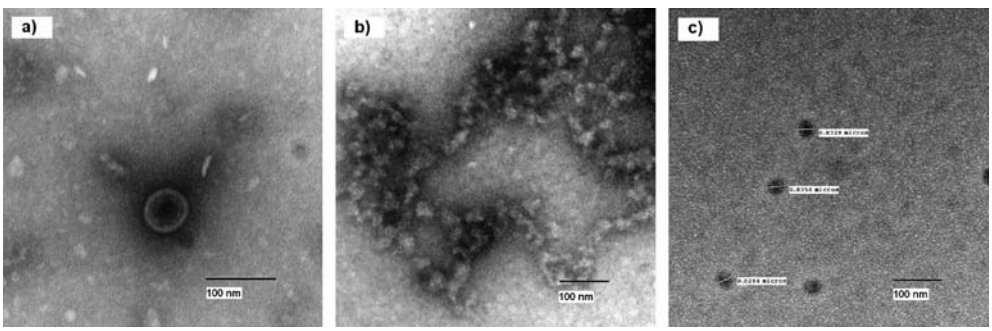

Fig. 2 TEM image of untreated and treated φ-X174 virus.

Table 5 Log reduction of PRD1 virus by NA–Al_2O_3 Plus, NA–TiO_2 and NA–CeO_2 adducts (20 mg mL^{-1})

	Contact time/min			Contact time/min			Contact time/min	
Nanoparticle formulation	5	30	Nanoparticle formulation	5	30	Nanoparticle formulation	5	30
Phage control	10.39	10.39	Phage control	10.39	10.39	Phage control	−10.39	−10.39
NA–CeO_2	T.n.t.c.[a]	T.n.t.c.	NA–Al_2O_3	T.n.t.c.	T.n.t.c.	NA–TiO_2	T.n.t.c.	T.n.t.c.
NA–CeO_2/Cl_2	T.n.t.c.	T.n.t.c.	NA–Al_2O_3/Cl_2	n.c.r.[b]	n.c.r.	NA–TiO_2/Cl_2	T.n.t.c.	T.n.t.c.
NA–CeO_2/Br_2	T.n.t.c.	T.n.t.c.	NA–Al_2O_3/Br_2	−10.39	−10.39	NA–TiO_2/Br_2	T.n.t.c.	T.n.t.c.
NA–CeO_2/I_2	T.n.t.c.	−10.39	NA–Al_2O_3/I_2	−10.39	−10.39	NA–TiO_2/I_2	−8.05	−10.39
NA–CeO_2/ICI	T.n.t.c.	−8.04	NA–Al_2O_3/ICI	T.n.t.c.	−10.39	NA–TiO_2/ICI	−10.39	−10.39
NA–CeO_2/IBr	−7.74	−10.39	NA–Al_2O_3/IBr	−10.39	−10.39	NA–TiO_2/IBr	−10.39	−10.39
NA–CeO_2/ICl_3	T.n.t.c.	−8.47	NA–Al_2O_3/ICl_3	−6.86	−10.39	NA–TiO_2/ICl_3	−10.39	−10.39

[a] T.n.t.c.. = too numerous to count. [b] N.c.r. = non consistent results.

stranded DNA virus (ds-DNA), containing a lipid layer underneath the viral capsid.[18] The lipid layer consists of phosphatidylethanolamine, phosphatidylglycerol and cardiolipin. PRD-1 has icosahedral protein capsid symmetry and infects Gram-negative bacteria such as *E. coli* and *Salmonella enterica*.[19] The capsid is approximately 70 nm in diameter and the mature virion has a molecular mass of about 66×10^6 Da.[20]

An initial concentration of 20 mg nanoparticles per mL of buffer solution was used to determine if the nanoparticles were effective against PRD-1. The initial results against MS2 and φ-X174 were promising, but PRD-1 has been reported to be very resistant to halogen treatment.[16] Table 5 shows the results using the different adducts of NA–Al_2O_3 Plus, NA–TiO_2 and NA–CeO_2 against the coliphage PRD-1 using a nanoparticle concentration of 20 mg mL^{-1}. A complete destruction of the PRD1 phage during 30 min of interaction for all the interhalogenated adducts of NA–Al_2O_3 Plus as well as for the brominated and iodinated adducts was observed. The chlorinated adduct gave inconsistent results during the set of experiments. Further, it is immediately clear that the NA–CeO_2 adducts were not as effective against this phage as the NA–Al_2O_3 Plus adducts. During a 5 min contact time, only the IBr adduct showed some activity; however during the 30 min interactions all of the interhalogenated adducts and the iodinated adduct had some activity. Only the I_2 and IBr adducts, however, displayed a complete inactivation of the PRD-1 phage during 30 min of interaction. The NA–TiO_2 adducts seem to have a better activity against the phage as compared to the NA–CeO_2 adducts. All the interhalogenated adducts and the iodinated adducts display some activity or a complete inactivation of the phage during 5 min of contact time. The chlorine and bromine adducts do not appear to be effective even after 30 min of contact time using this concentration of 20 mg mL^{-1}. The same is true for the activated TiO_2.

Table 6 displays the results using the lower nanoparticle concentration of 10 mg mL^{-1} and it can be seen that the brominated adduct of alumina was no longer active against the PRD-1 phage. The reason for the better results obtained using this lower nanoparticle concentration for the ICl and ICl_3 adduct of NA–Al_2O_3 Plus during the 5 min interaction is unknown. NA–CeO_2/I_2 was also no longer effective at this concentration and the IBr adduct was still the most efficient in the cerium oxide series, displaying a complete inactivation of the phage at 30 min (higher than log 10 reduction) and higher than a 7 log reduction in 5 min. The activities for the NA–TiO_2 adducts appear to be very similar to those using a nanoparticle concentration of 20 mg mL^{-1}, displaying good activities for the interhalogen adducts as well as for the iodinated adduct. The standard deviation values for the PRD-1 testings were ±1 log for the ones that did not display a complete inactivation.

The results obtained using PRD-1 phage clearly reveal some differences using the various metal oxide nanoparticles, although some results were more difficult to reproduce. The adducts prepared from NA–Al_2O_3 Plus appear to be the most efficient overall. It is also clear that the chlorinated and brominated adducts were not very active except for the Br_2 adduct of NA–Al_2O_3 Plus. The adducts prepared from NA–CeO_2 appear to have the lowest activity against the PRD-1.

Table 6 Log reduction of PRD1 virus by NA–Al_2O_3 Plus, NA–TiO_2 and NA–CeO_2 adducts (10 mg mL^{-1})

	Contact time/min			Contact time/min			Contact time/min	
Nanoparticle formulation	5	30	Nanoparticle formulation	5	30	Nanoparticle formulation	5	30
Phage control	10.39	10.39	Phage control	10.39	10.39	Phage control	10.39	10.39
NA–CeO_2	T.n.t.c.[a]	T.n.t.c.	NA–Al_2O_3	T.n.t.c.	T.n.t.c.	NA–TiO_2	T.n.t.c.	T.n.t.c.
NA–CeO_2/Cl_2	T.n.t.c.	T.n.t.c.	NA–Al_2O_3/Cl_2	T.n.t.c.	T.n.t.c.	NA–TiO_2/Cl_2	T.n.t.c.	T.n.t.c.
NA–CeO_2/Br_2	T.n.t.c.	T.n.t.c.	NA–Al_2O_3/Br_2	T.n.t.c.	T.n.t.c.	NA–TiO_2/Br_2	T.n.t.c.	T.n.t.c.
NA–CeO_2/I_2	T.n.t.c.	T.n.t.c.	NA–Al_2O_3/I_2	−10.39	−10.39	NA–TiO_2/I_2	−10.39	−10.39
NA–CeO_2/ICI	T.n.t.c.	−8.35	NA–Al_2O_3/ICI	−10.39	−10.39	NA–TiO_2/ICI	−8.49	−10.39
NA–CeO_2/IBr	−7.4	−10.39	NA–Al_2O_3/IBr	−10.39	−10.39	NA–TiO_2/IBr	−10.39	−10.39
NA–CeO_2/ICl_3	−7.11	T.n.t.c.	NA–Al_2O_3/ICl_3	−10.39	−10.39	NA–TiO_2/ICl_3	−7.82	−10.39

[a] T.n.t.c.. = too numerous to count.

4. Conclusions

Nanoparticles hold promise as disinfectants against different viruses, including the bacteriophages MS2, φ-X174, and PRD-1. Although scant data exists in the literature regarding the use of nanomaterials against viruses we have now found that successful results can be obtained using halogenated and interhalogenated metal oxide nanoparticles.

As supported by the research performed by Brion *et al.*[16] we have also found that the order of resistance against halogen treatment increases in the order of MS2 < φ-X174 < PRD-1. PRD-1 is lipid-containing, which further increases its resistance against chemical treatment. In general, we found that the interhalogenated adducts were the most promising candidates for phage inactivation, however, the iodine adducts also proved to be very efficient. The chlorinated adducts did not perform very well; only in the case of MS2 phage did the NA–Al_2O_3 Plus adduct have some activity. The brominated adducts performed slightly better, displaying activity against MS2 phage in all the prepared metal oxide adducts, and activity against the other two phages, φ-X174 and PRD-1 in some instances. The activated nanoparticles themselves did not display any significant activity against any of the three phages studied.

Overall, the NA–Al_2O_3 Plus adducts were outstanding in performance and exceeded the performance of the NA–CeO_2 adducts. The activities of the NA–TiO_2 adducts were close to those prepared from NA–Al_2O_3 Plus, or better in a few cases. The generally lower activities of the NA–CeO_2 adducts can probably be explained by the lower amounts of halogen/interhalogen adsorbed on the surface and by the fact that cerium oxide has a high molar mass, and so for a given mass fewer nanoparticles. Another observation was that Al_2O_3 and TiO_2 materials remained suspended in the aqueous medium for longer periods of time, leading to more extended interaction with the phage, further increasing their activities.

The mechanism by which these nanoparticles operate is not completely known at this time, but reasons for the excellent activity could include their abrasive character, caused by their high surface area and many corners, edges and defect sites as well as the oxidative power of the halogens/interhalogens.[14b] Further studies, including resin-embedded TEM images may give more insight to the mechanism.

Based on these results, nanoscale metal oxide–halogen adducts as antimicrobials will have applications in a variety of settings such as in hospitals and in protection against bioterrorism threats.

Acknowledgements

We would like to thank Dr A. Lorena Passarelli for the use of her microscope. The Division of Biology and Dr Dan Boyle at Kansas State University are acknowledged with gratitude for use and assistance of their TEM. The support of the KSU Targeted Excellence Program and the Army Research Office are acknowledged with gratitude.

References

1 O. B. Koper, J. S. Klabunde, G. L. Marchin, K. J. Klabunde, P. Stoimenov and L. Bohra, *Curr. Microbiol.*, 2002, **44**, 49–55.
2 C. J. Yu, J. Lin, *U.S Pat. Appl. Publ.*, 2004.
3 A. R. Bender, H. Von Briesen, J. Kreuter, I. B. Duncan and H. Rubsamen-Waigmann, *Antimicrob. Agents Chemother.*, 1996, **40**, 1467–1471.
4 T. Hamouda, A. Myc, B. Donovan, A. Y. Shih, J. D. Reuter and J. R. Baker, *Microbiol. Res.*, 2001, **156**, 1–7.
5 R. Sommer, W. Pribil, S. Pfleger, T. Haider, Werderitsch and P. Gehringer, *Water Sci. Technology.*, 2004, **50**, 159–164.
6 E. R. Blatchley, W.-L. Gong, J. E. Alleman, J. B. Rose, D. E. Huffman, M. Otaki and J. T. Lisle, *Water Environ. Res.*, 2007, **79**, 81–92.
7 R. Pedahzur, D. Katzenelson, N. Barnea, O. Lev, H. I. Shuval, B. Fattal and S. Ulizur, *Water Sci. Technol.*, 2000, **42**, 293–298.
8 N. A. Chowdhary Brit. UK Pat. 2002, 7 pp.
9 Y. S. Malik and S. M. Goyal, *Int. J. Food Microbiol.*, 2006, **109**, 160–163.
10 B. L. T. Lau, G. W. Harrington, M. A. Anderson and I. Tejedor, *Water Sci. Technol.*, 2004, **50**, 223–228.
11 F. Tepper, L. Kaledin and C. Hartmann, *Advances in Filtration & Separation Media*, 2004, 110–123.
12 G. M. Brion and J. Silverstein, *Water Res.*, 1999, **33**, 169–179.
13 M. E. Alvarez and R. T. O'Brien, *Appl. Environ. Microbiol.*, 1982, **44**, 1064–1071.
14 (*a*) P. K. Stoimenov, V. Zaikovski and K. J. Klabunde, *J. Am. Chem. Soc.*, 2003, **125**, 12907–12913; (*b*) P. K. Stoimenov, G. L. Klinger and K. J. Klabunde, *Langmuir*, 2002, **18**, 6679–6686.
15 C. K. Mathews *Bacteriophage Biochemistry*, New York, NY, 1971.
16 G. M. Brion, N. B. O'Banion and G. L. Marchin, *J. Water and Health*, 2004, **2**, 261–266.
17 J. A. Häggström, P. K. Stoimenov and K. J. Klabunde, *Chem. Mater.*, 2008, **20**, 3174–3183.
18 J. T. Huiskonen and S. J. Butcher, *Curr. Opin. Struct. Biol.*, 2007, **17**, 229–236.
19 J. T. Huiskonen, V. Manole and S. J. Butcher, *Proc. Natl. Acad. Sci. U. S. A.*, 2007, **104**, 6666–6671.
20 S. Fuller, *Structure*, 2005, **13**, 1738–1739.

